SCINTILLATING FIBERS

Presented by L. Poggioli

Contributions from : R. De Salvo, A. Henriques, L. Linssen, M. Sivertz, and R. Wigmans

We report on the use of scintillating fibers in calorimetry for LHC. We will first review the major advantages of combining lead and fibers, then look at the different approaches, with emphasis on the one used by the SPACAL group at CERN. We will present the most significant results (SPACAL), and finally review what is needed to move to a full LHC calorimeter.

1 Conceptual designs

1.1 Choice of lead and fibers

Between the two possibilities for a dense absorber, i.e. lead or uranium, the first has many advantages with respect to the LHC requirements. Lead in association with scintillators can provide compensation [1,2], it is faster than uranium (the neutrons thermalizing primarily via elastic scattering off protons, which is a fast process), and the neutron yield is 3 times less than in uranium, which greatly reduces the radiation damage caused by neutrons. Moreover, lead is rather cheap, abundant, and easy to machine. Finally, used with scintillators, it is as compact as uranium (if one requires compensation).

Using fibers leads to the well known advantages of scintillators, with some specific additional features : fibers allow a very fine sampling, which can provide good energy resolution, and arbitrarily fine granularity. Most importantly one does not need external wave length shifters or light guides, hence the use of fibers provides fast signals, significant light yield ($\simeq 10^3$ photoelectrons per incident GeV), and an almost perfect hermeticity. This implies having the fibers run approximately in the direction of the incident particles.

If clearly this association can reach most of the requirements for a LHC calorimeter, it raises some difficult problems : non-gaussian response at low incidence angles, uniformity problems due to fiber-to-fiber fluctuations and finite attenuation length, difficulty achieving longitudinal sampling, and the need for radiation hardness.

1.2 Different approaches

To tackle these problems different approaches are being tested, mainly in the US and at CERN. Since the Americans (grouped into the funded subsystem proposal PC-020) are still at an early stage, we will concentrate on the SPACAL approach at CERN, under the direction of Richard Wigmans.

The basic design consists of a matrix made up of extruded lead plates which are soldered together with tin, in which $1\,mm$ diameter fibers are embedded. At

this stage of the project, the modules are hexagonal (side $43.3mm$), the distance between fibers (center-to-center) being $2.2\,mm$. The lead to fiber ratio in volume is set to $4:1$ to achieve compensation.
This leads to the following parameters, which give a very compact calorimeter, a radiation length $X_0 = 0.75\,cm$, and an interaction length $X_{int} = 21\,cm$.

Among the various prototypes which have been tested, the most recent consisted of 155 modules, each $2\,m$ long ($\simeq 9.5\,X_{int}$), representing a effective volume of $13.3\,tons$ ($2\,mX2\,mX1\,m$).
For these tests, SCSN-38 fibers from Kyowa Gas Company (Japan) were used. Each fiber was equipped with an aluminium mirror (sputtering technique), with a very good reflection coefficient ($R = 85\%$).
The fibers, sticking out at the end, were bunched together, then coupled via an hexagonal light guide to a photomultiplier. A yellow filter was also used, which in conjunction with the mirror increased the effective attenuation length λ_{att} to about $8\,meters$.
A schematic description of this approach can be found in Fig. 1.

2 Performances

2.1 Major results (SPACAL)

We review here the most significant results on uniformity, electron and hadron response.
Fig. 2 shows the results of a electron scan across 2 modules. The electron signal is more sensitive to fiber-to-fiber fluctuation than with hadrons, since less fibers are involved in the shower development. One observes a uniformity of better than 1% (2% between the modules).

Fig. 3 shows the electron resolution versus the shooting angle θ_z, assuming an expression $\sigma/E = a + b/\sqrt{E}$. One obtains a scaling term of the order of 13%. The constant term, much more sensitive to θ_z, is as low as 1%, for angles around $3\,degrees$, which does not spoil the projectivity.

Fig. 4 gives the impact point resolution for electrons and pions, using traditional barycenter methods. At $80\,GeV$, the average resolution is of $1.6\,mm$ in each direction for electrons, which is quite satisfactory, with regard to the bad granularity of the prototype for electrons. For pions, the average resolution is around $5\,mm$ in each direction.

Fig. 5 shows the energy resolution for individual hadrons in the range $5 - 150\,GeV/c$ (preliminary). Assuming the same expression as for electrons leads to a scaling term of 29% and a constant term of 2.6%. This rather high constant term reflects first a very short attenuation length in the fibers close to the photomultiplier coming from light propagating in the cladding and affecting deeply penetrating hadrons only. This effect is under study and can be easily corrected. Second, the finite attenuation length in the fiber, which affects the uniformity in depth, also contributes. Anyway, this effect should be less important for jets. It seems that one could bring this constant term down to the 1% level.

We move now to the time structure and speed of the signals. Fig 6 gives the resolution for electrons and hadrons versus the integration time (preliminary). One can clearly use a very short gate length (of the order of $30\,ns$) to get a satisfactory response. The same holds for the e/h ratio (Fig. 7), which also shows that the calorimeter is slightly undercompensating ($e/h \simeq 1.05$. Preliminary).

An other important highlight of this technique is its extreme compactness as shown in Fig. 8, where one sees that an integration radius of $30\,cm$ is sufficient to provide a stable hadronic response.

2.2 Electron-pion separation

In this section, we discuss different ways of separating electrons from *isolated* pions. What is relevant for the LHC is the separation from jets and is under study.

A first method exploits the high speed of the signals and their intrinsic time structure [3]. As shown in Fig. 9, measuring the width of the signal at $20\% - 20\%$ yields a rejection factor of 800 for an electron efficiency of 99% at $80\,GeV$. This method could be easily used at a first level trigger.

A more conventional method based on lateral profile of the shower leads to (in conjunction with a preshower detector) a rejection factor of 5000 at $80\,GeV$ for an electron efficiency of 98%. This method could also be implemented at a first level trigger.

Due to the very fine granularity of the calorimeter for hadrons, it is possible to identify an electron (with 95% efficiency), for a hadron misidentification of 10^{-3}, when the 2 particles are as close as $4.3\,cm$.

All these results can be found in more detail in [4,5,6].

2.3 Radiation damage

This crucial issue is being studied by many groups [7], in particular in the SPACAL group [8]. The goals are manifold : with studying different types of fibers, with different types of irradiation (neutrons, photons, electrons), in different atmospheres (air, oxygen, nitrogen).

If one parametrizes the light emission of a fiber as a function of the distance d to the photomultiplier, by the expression : $I(d) = I_0 e^{-d/\lambda_{att}}$, the radiation has 2 effects . First, it affects the emission I_0, i.e. a 20% decrease after $10 Mrad$ (this stands for 3HF+PTP fibers), and second the transmission which is less critical. Fig. 10 shows a typical response for 2 kinds of fibers to non-homogeneous irradiation in depth, simulating the damage due to π^0's.

Using actual characteristics of the fibers these effects lead to a degradation of the order of 1.5% on calorimeter performances, as evaluated by Monte-Carlo (on electron linearity, electron resolution).

Considering now what it means for a calorimeter in a LHC environment, one should concentrate on the damage due to π^0's, which is dominant and very localized in depth. The damage caused by charged hadrons is less important since it is spread

over the full length of the fibers. The damage caused by neutrons is almost negligible (with minimal neutron yield for the Pb/fiber combination, and electronics sitting after $10\,X_{int}$).
In conclusion, $10\,Mrad$ corresponds to 4 years running at a rapidity of $\eta = 2.8$, for a luminosity of $10^{34}\,cm^{-2}s^{-1}$, at a distance of $4\,meters$ from the vertex. The situation is not critical, but still requires a lot of effort, mainly to find a solution for rapidities larger than 3.

3 Towards a real LHC calorimeter

The question is what still has to be done in order to be ready to start building a full calorimeter for LHC in about 2 years.

A major issue concerns calibration, the aim being to work at the 1% level. The problem at LHC will be made more critical because it will be difficult to calibrate modules in test beams, and because of the eventual shifts in performance caused by radiation. Of course one should take advantage of the experience from previous experiments (UA2, CDF, ZEUS).
A lot of work has to be done on this point.

Concerning radiation damage issues, more tests are needed with new fibers and in conditions closer to an LHC environment (long fibers in lead put in real beams). Once more one has to emphasize the necessity to find a solution for rapidities greater than 3.

Concerning the production of modules, even though the current extrusion technique is quite promising (SPACAL), it needs to be improved in order to be mass produced ($\simeq 10^5$ modules).
Moreover, one has to move to projective modules for a final configuration. This will lead to a better matched granularity for electrons, and could provide longitudinal sampling, if one can read out separately long and short (i.e. starting after roughly $30\,X_0$) fibers.

As for light detection devices, photomultipliers are not optimal, mainly because of their limited dynamic range and power consumption ($\simeq 1W$). In that respect, a new device has been developed in the SPACAL group, the Hybrid Photo Diode (Fig. 11). This device provides a good dynamic range (10^5), low power consumption ($\simeq mW$), and allows for anode segmentation to match the required granularity for electrons. This is under study. The behavior in a magnetic field has to be investigated.

A lot of effort has to be directed towards trigger and acquisition issues. Since most of these aspects are not specific to the fiber technique, one should concentrate on its unique features (electron identification at prompt trigger level).

A last point which needs work is full-scale engineering. One needs to maintain a projective structure of about 10^4 tons, without spoiling hermeticity. This problem is being undertaken by many groups (by EMPACT and TEXAS in The United States and SPACAL at CERN).

We describe here a basic design (SPACAL). The detector is divided into independent structures called "super-rings" (Fig. 12) to give easier handling and better access to the central part of the detector. Each "super-ring" is in turn made out of rings, themselves built out of pyramidal modules. All these elements are maintained together using glue and iron skirts, and reinforced by a honeycomb structure. CAD studies are in progress.

In parallel, robots for inserting the fibers into the modules are being developed. A different solution is under study for the very forward region.

4 Conclusions

The fiber technique for calorimetry at hadron colliders was introduced around three years ago. It is already very advanced, many non trivial problems having been already solved (mainly in the SPACAL group).
Up to now, no problem looks impossible to solve, but a big effort on *R&D* is still needed (mechanics, calibration).

We conclude with two remarks :
The scintillating fiber technique provides an integrated electromagnetic AND hadronic calorimeter.
With its features (fast, hermetic, uniform, good electromagnetic and hadronic resolution, granularity), this calorimeter can provide valuable and unbiased information (for electrons, jets, missing E_T) already at the first level trigger, which will be of crucial importance for extracting the physics at the LHC.

References

[1] R. Wigmans, Nucl. Instr. and Meth. **A259** (1987) 389.

[2] E. Bernardi et al., Nucl. Instr. and Meth. **A262** (1987) 229.

[3] R. DeSalvo at al., Nucl. Instr. and Meth. **A279** (1989) 467.

[4] D. Acosta et al., Results of prototype studies for a spaghetti calorimeter, Nucl. Instr. and Meth. **A294** (1990) 193.

[5] D. Acosta et al., Electron-pion discrimination with a scintillating fiber calorimeter, CERN/LAA/HC 90-008, to be published in Nucl. Instr. and Meth.

[6] D. Acosta et al., Localizing particles showering in a spaghetti calorimeter (in preparation).

[7] Proceedings of the Workshop on Radiation Damage of Plastic Scintillators, Tallahassee (1990).

[8] D. Acosta et al., Effects of radiation damage on scintillating fiber calorimetry (in preparation).

Figure Captions

1. An electromagnetic module. (SPACAL)
2. Uniformity scan for 80 GeV electrons across modules (SPACAL)
3. Electromagnetic resolution versus the shooting angle θ_z (SPACAL).
4. Position resolution for 80 GeV electrons and pions versus distance from the center of a module (SPACAL).
5. Energy resolution for $5 - 150\, GeV \pi^-$. Preliminary results (SPACAL).
6. Electromagnetic and hadronic energy resolution as a function of the gate width. Preliminary results (SPACAL).
7. e/h ratio as a function of the gate width. Preliminary results (SPACAL).
8. Hadronic resolution for isolated π^- versus the integration radius. Preliminary results (SPACAL).
9. Distribution of the widths, measured at 20% of the amplitude, of e.m. and hadronic shower signals at 80GeV (SPACAL).
10. Response of 2 kinds of fibers to different irradiation doses. The dose is non-homonogeneous in depth to simulate the damage from π^0's.
11. Layout of a Hybrid Photo Diode with anode segmentation (DEP Company & SPACAL).
12. Layout of a full coverage fiber calorimeter with projective geometry, organized in "super-rings" (SPACAL).

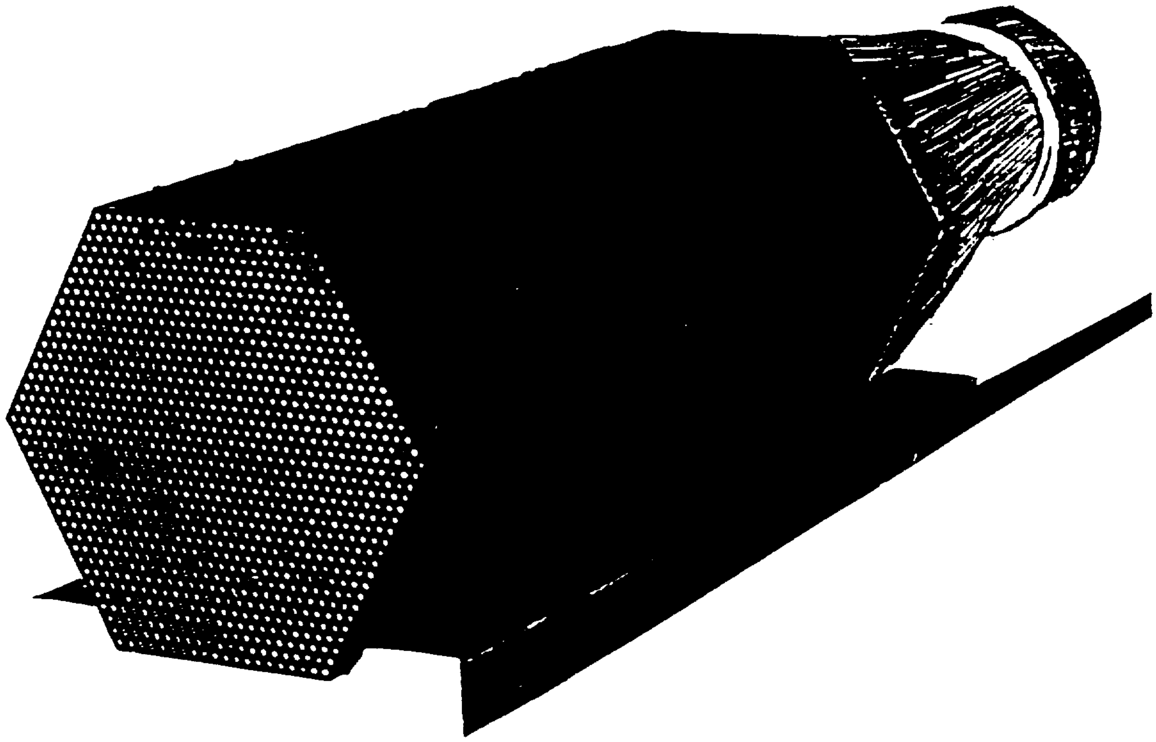

Fig. 1

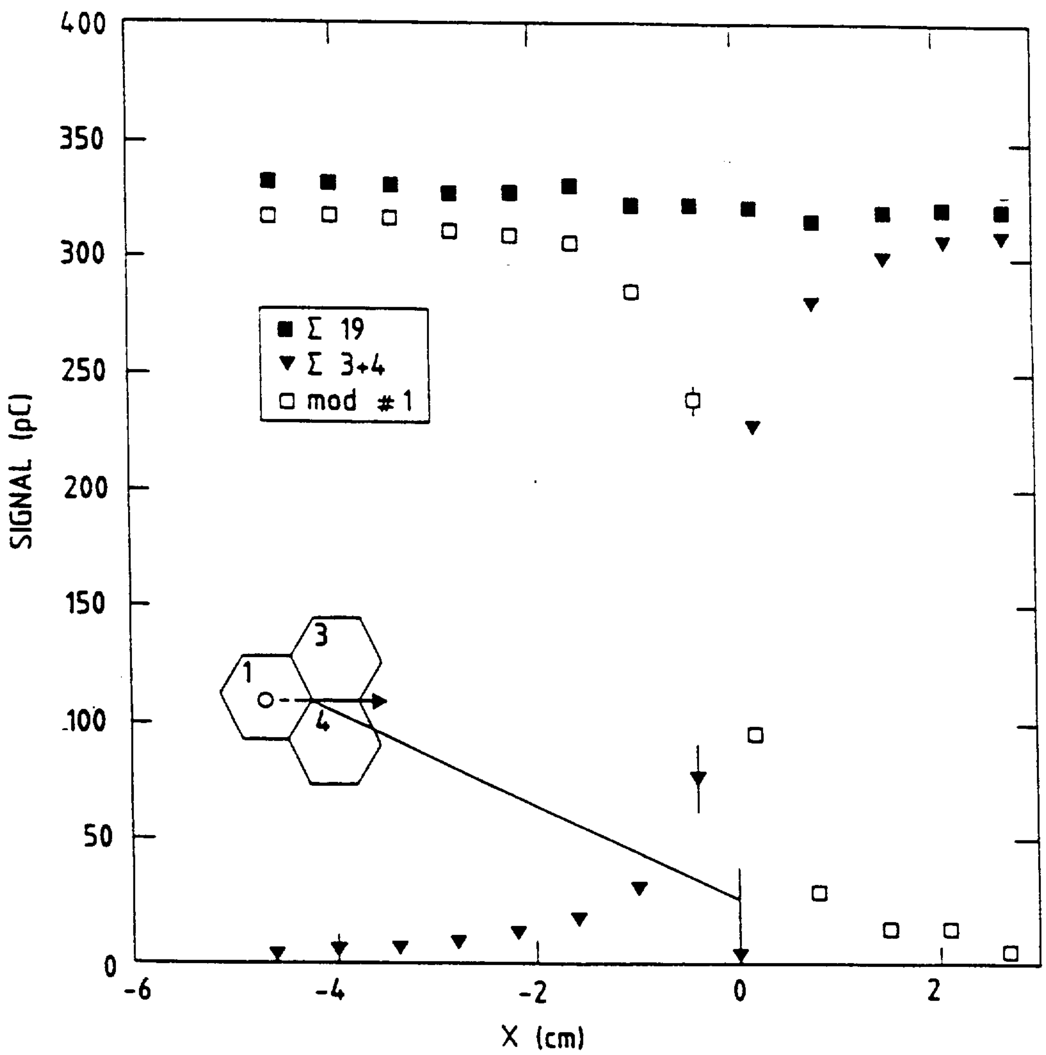
SIGNAL (pC)
X (cm)
Σ 19
Σ 3+4
mod #1
1
3
4
400
350
300
250
200
150
100
50
0
-6
-4
-2
0
2

Fig. 2

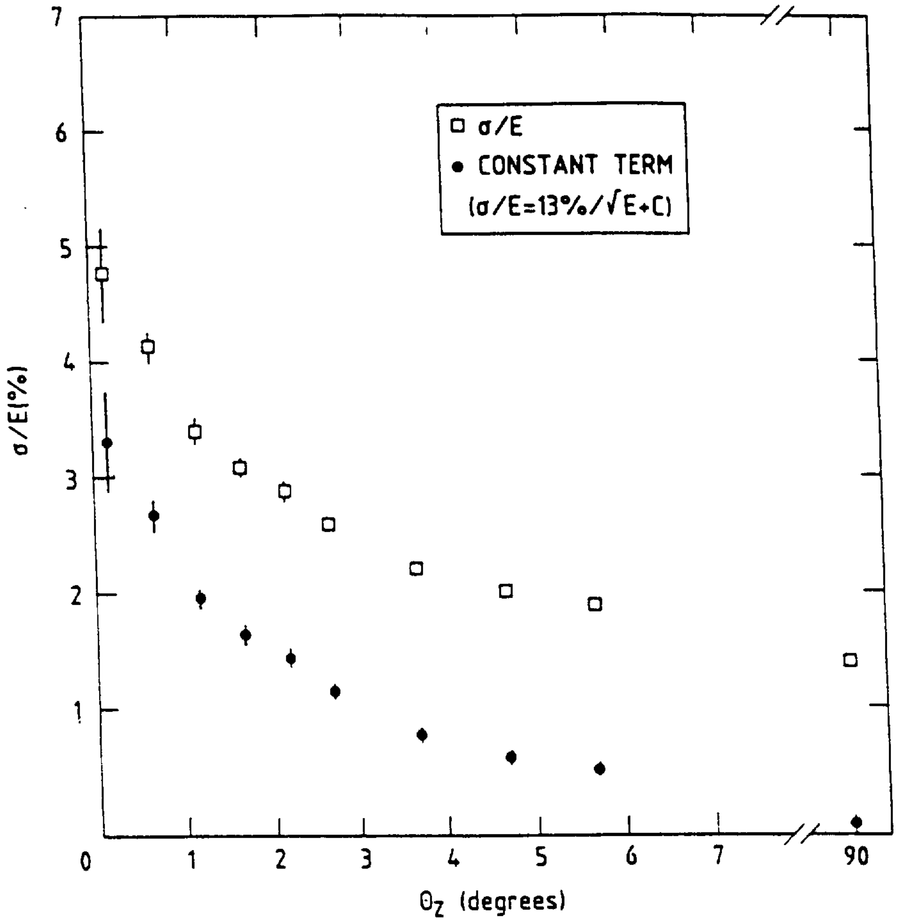
σ/E
CONSTANT TERM
(σ/E=13%/√E+C)
σ/E(%)
θZ (degrees)
0
1
2
3
4
5
6
7
90

Fig. 3

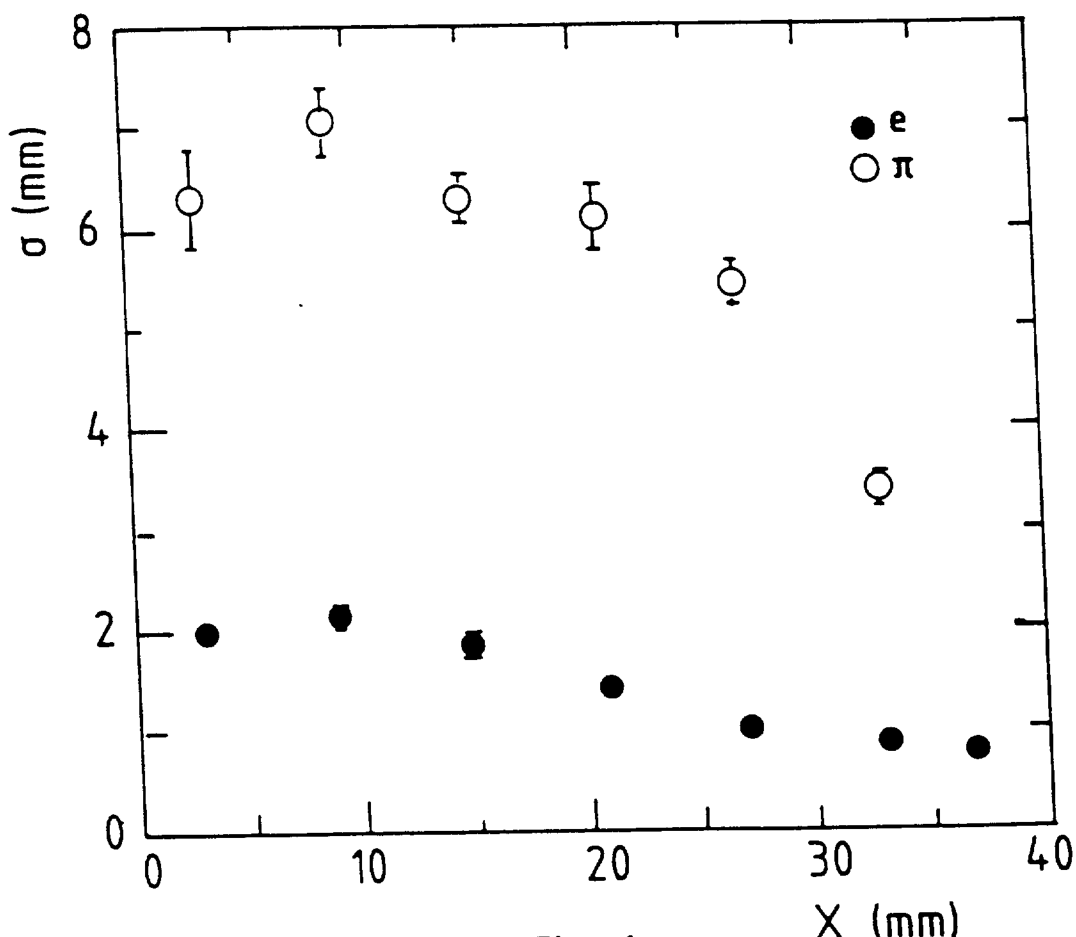
e
π
σ (mm)
X (mm)
0
2
4
6
8
10
20
30
40

Fig. 4

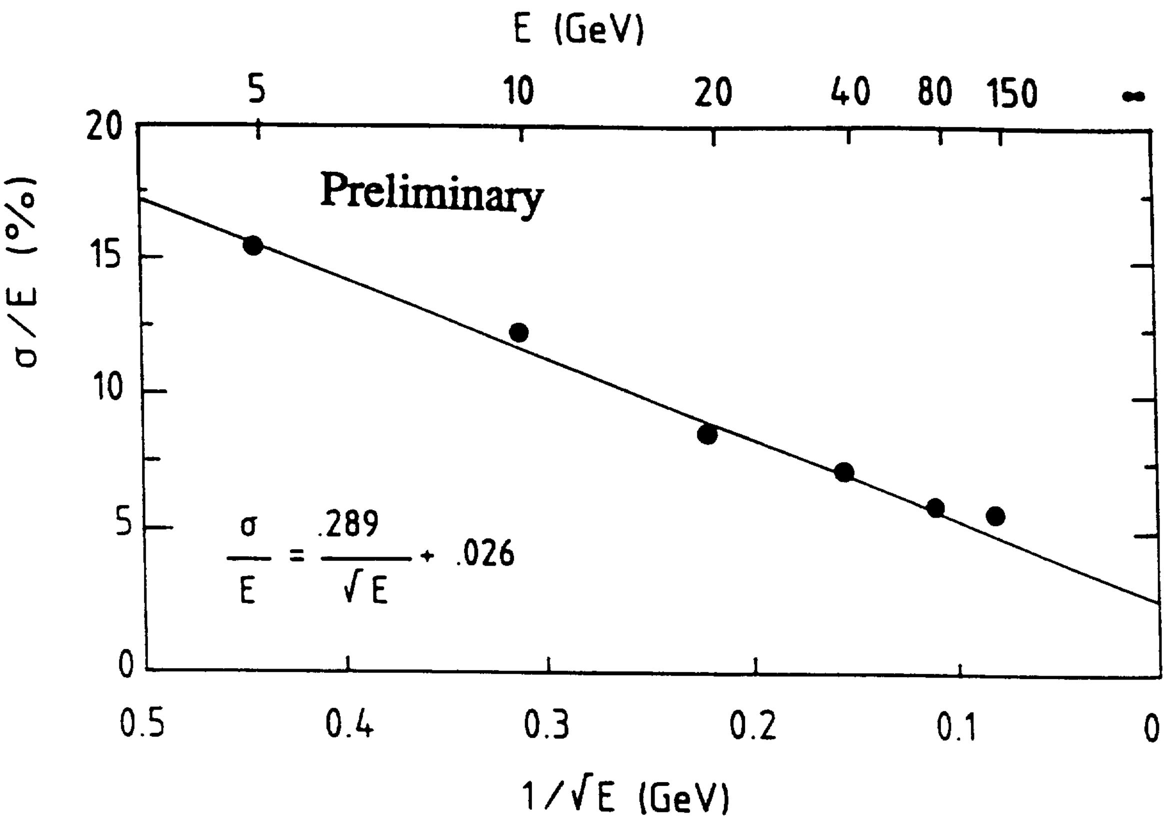
E (GeV)
5
10
20
40
80
150
∞
20
15
10
5
0
σ/E (%)
Preliminary
σ/E = .289/√E + .026
0.5
0.4
0.3
0.2
0.1
0
1/√E (GeV)

Fig. 5

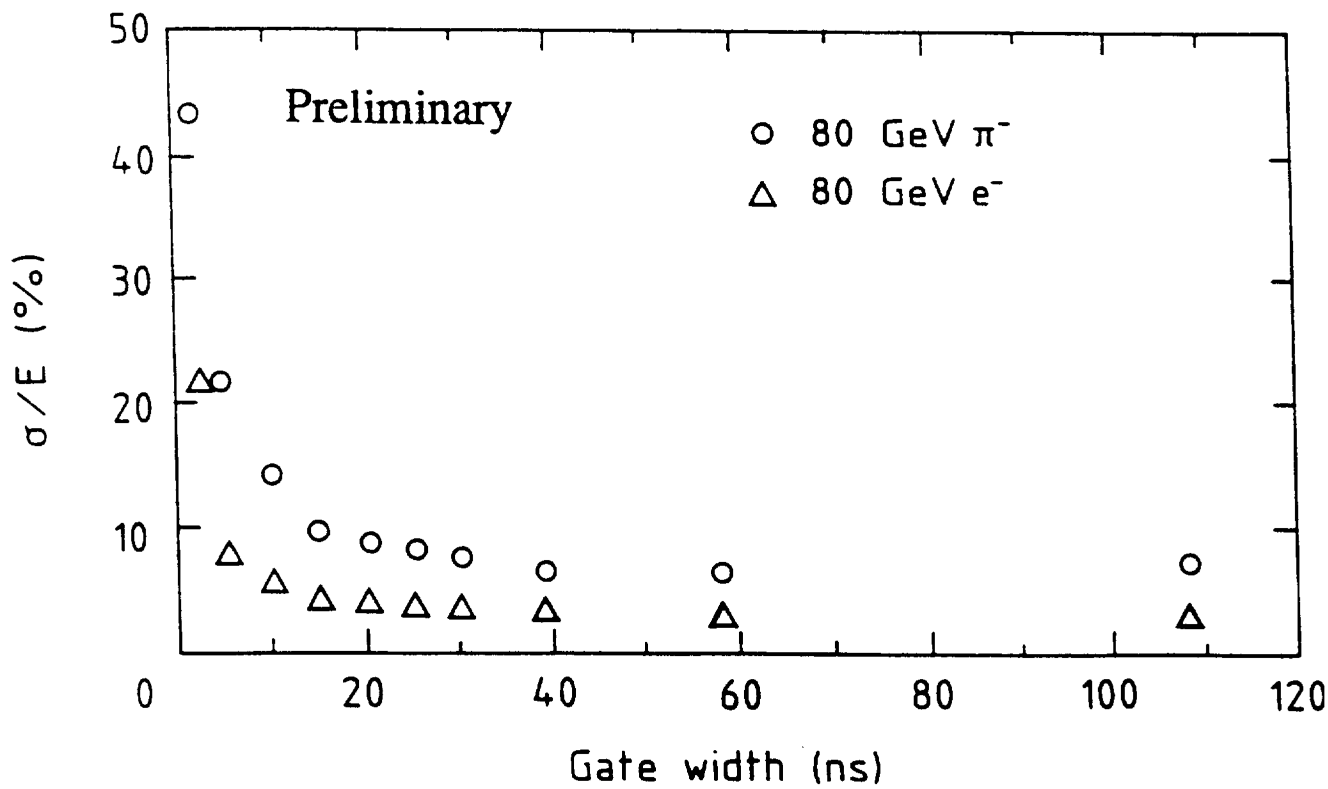
50
40
30
20
10
0
σ/E (%)
Preliminary
80 GeV π⁻
80 GeV e⁻
20
40
60
80
100
120
Gate width (ns)

Fig. 6

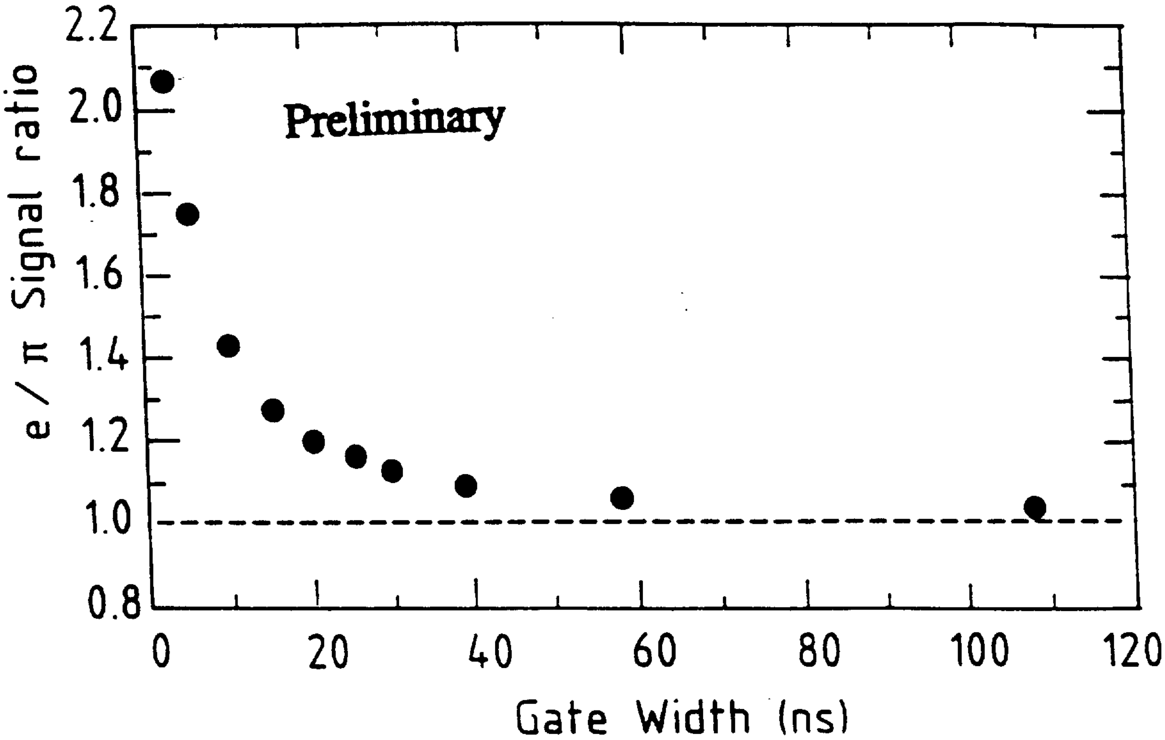
Preliminary
e / π Signal ratio
2.2
2.0
1.8
1.6
1.4
1.2
1.0
0.8
0
20
40
60
80
100
120
Gate Width (ns)

Fig. 7

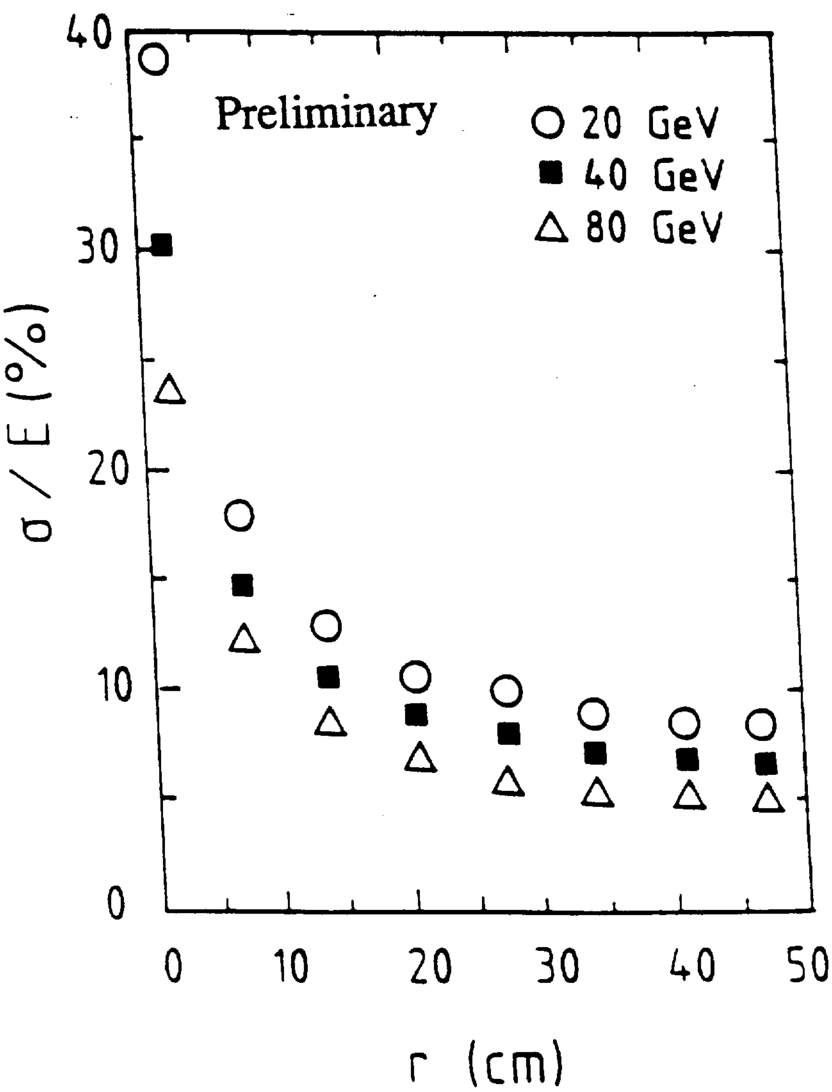
Preliminary
○ 20 GeV
■ 40 GeV
△ 80 GeV
σ / E (%)
40
30
20
10
0
0
10
20
30
40
50
r (cm)

Fig. 8

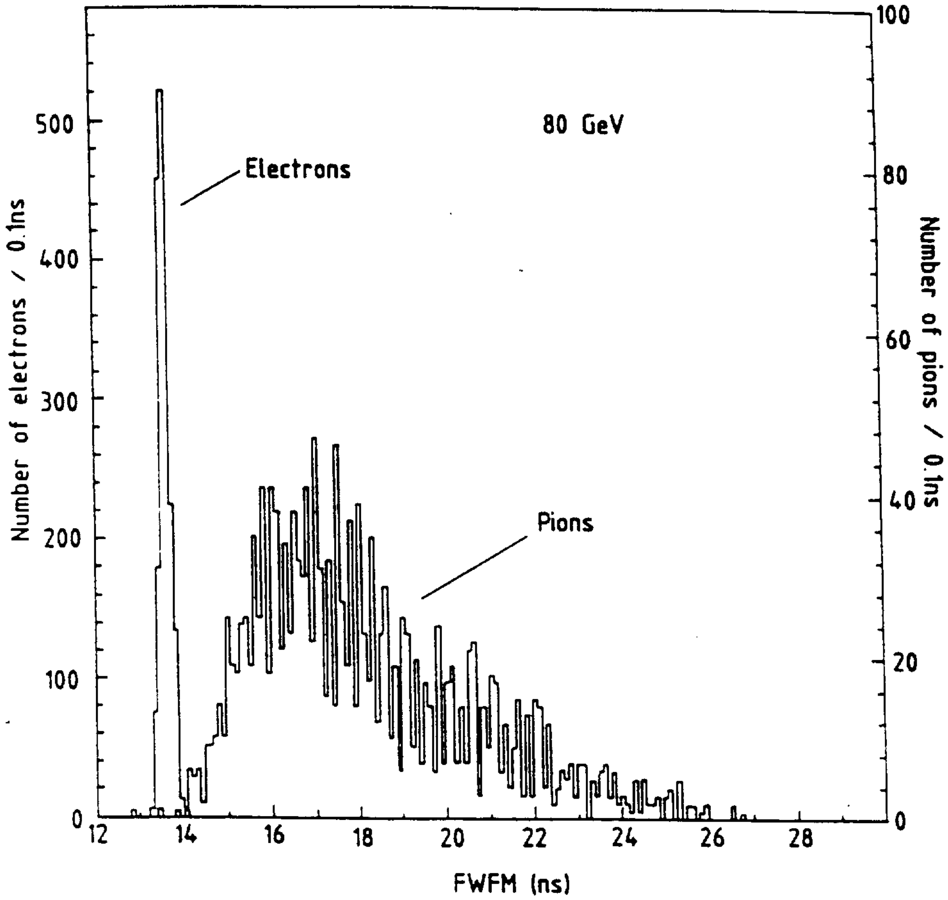
80 GeV
Electrons
Pions
Number of electrons / 0.1ns
Number of pions / 0.1ns
FWFM (ns)
0
100
200
300
400
500
0
20
40
60
80
100
12
14
16
18
20
22
24
26
28

Fig. 9

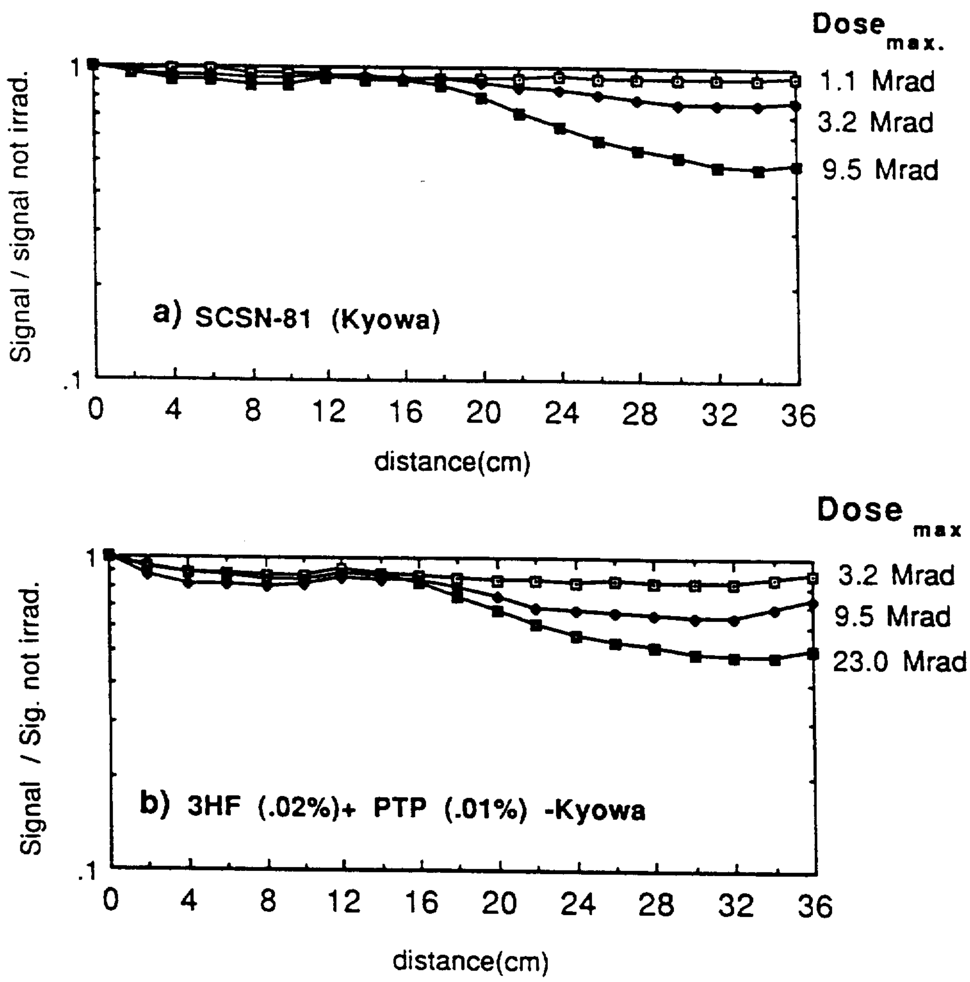
Dose max.
1.1 Mrad
3.2 Mrad
9.5 Mrad
a) SCSN-81 (Kyowa)
Signal / signal not irrad.
distance(cm)
1
.1
0
4
8
12
16
20
24
28
32
36
Dose max
3.2 Mrad
9.5 Mrad
23.0 Mrad
b) 3HF (.02%)+ PTP (.01%) -Kyowa
Signal / Sig. not irrad.
distance(cm)
1
.1
0
4
8
12
16
20
24
28
32
36

Fig. 10

MODULE 18/11E WITH PIXEL ARRAY

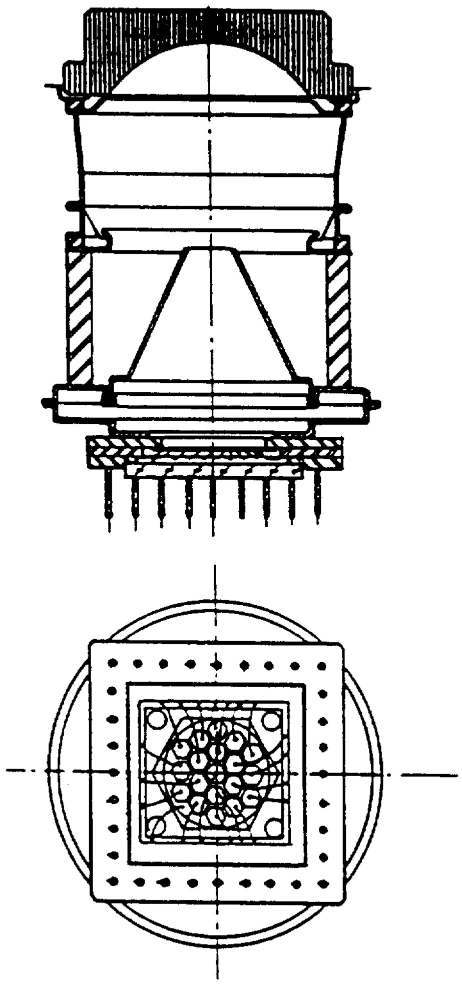

Fig. 11

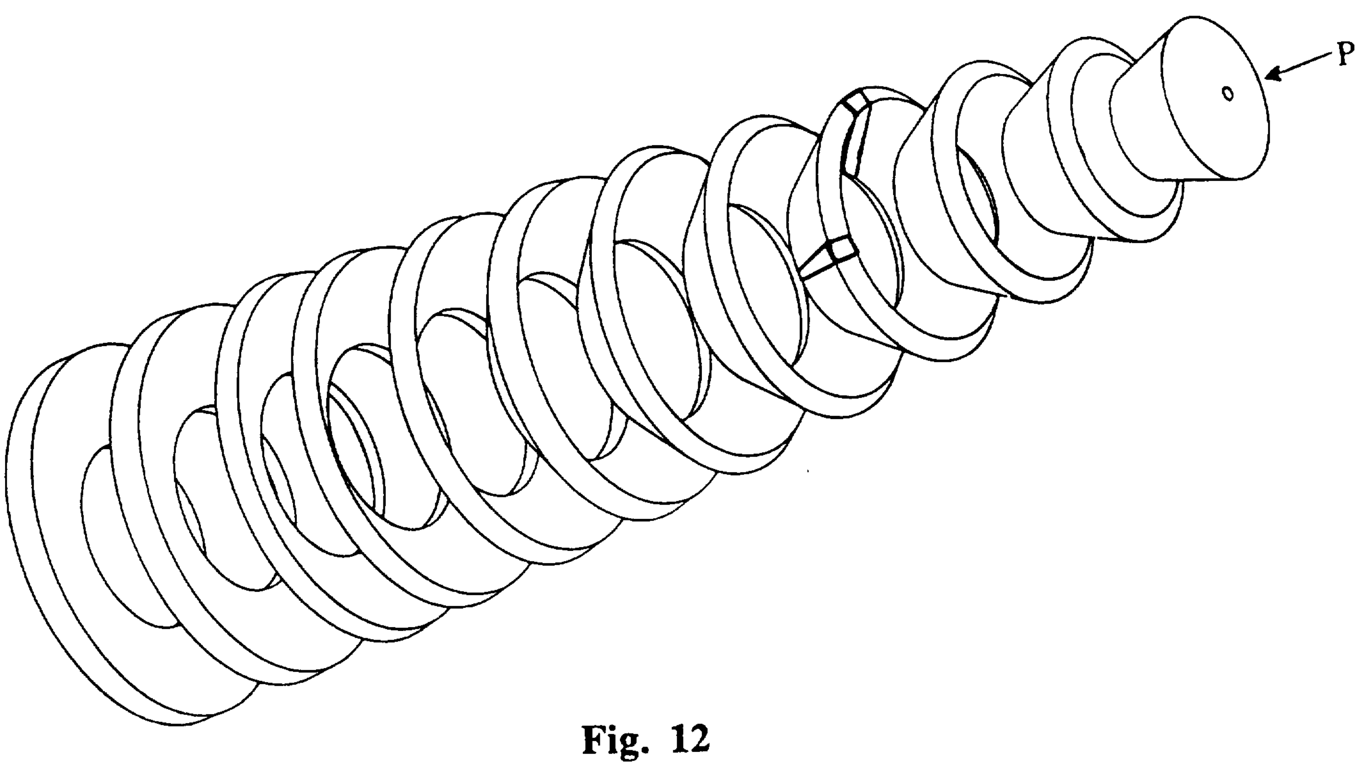

Fig. 12